

Reconciling cosmic ray diffusion with Galactic magnetic field models

G. Giacinti,^a M. Kachelrieß,^b D. V. Semikoz^{c,d}

^aMax-Planck-Institut für Kernphysik, Heidelberg, Germany

^bInstitutt for fysikk, NTNU, Trondheim, Norway

^cAPC, Universite Paris Diderot, CNRS/IN2P3, CEA/IRFU, Observatoire de Paris, Sorbonne Paris Cite, 119 75205 Paris, France

^dNational Research Nuclear University MEPhI (Moscow Engineering Physics Institute), Kashirskoe highway 31, 115409 Moscow, Russia

Abstract. We calculate the diffusion coefficients of charged cosmic rays (CR) propagating in regular and turbulent magnetic fields. If the magnetic field is dominated by an isotropic turbulent component, we find that CRs reside too long in the Galactic disc. As a result, CRs overproduce secondary nuclei like boron for any reasonable values of the strength and the coherence length of an isotropic turbulent field. We conclude therefore that the propagation of Galactic CRs has to be strongly anisotropic because of a sufficiently strong regular field and/or of an anisotropy in the turbulent field. As a consequence, the number of sources contributing to the local CR flux is reduced by a factor $\mathcal{O}(100)$ compared to the case of isotropic CR diffusion.

Keywords: High energy cosmic rays, Galactic magnetic field.

Contents

1	Introduction	1
2	Theoretical framework	2
3	Diffusion tensor and magnetic field models	3
3.1	Pure isotropic turbulent field	3
3.2	Isotropic turbulence with a uniform regular field	4
3.3	Anisotropic turbulent field	6
4	Discussion	9
4.1	Number of sources contributing to the local CR flux	10
4.2	Additional evidence against a steady-state CR flux	11
4.3	Possible restrictions	11
5	Conclusions	12

1 Introduction

The propagation of Galactic cosmic rays (CR) is usually described by empirical diffusion models where the energy dependence of the diffusion coefficient $D(E) = D_0(E/E_0)^\beta$ is obtained fitting observations [1, 2]. In such models, discrete CR sources are approximated by a continuous distribution filling a disk with typical vertical height $h_d \sim 0.2$ kpc, while CRs diffuse in a CR halo of much larger height $h \sim 3-5$ kpc. Cosmic rays either interact or escape in the intergalactic space when they reach the boundary of the CR halo. The solutions to these diffusion models are derived typically in the steady-state regime, i.e. any time-dependence in the injection history of CRs is neglected.

An important constraint on these models comes from ratios of stable primaries and secondaries produced by CR interactions on gas in the Galactic disk, which depend on the grammage X crossed by CRs. In particular, the boron-to-carbon (B/C) ratio measured by the AMS-02 experiment has been interpreted by the collaboration as being consistent with a $\beta \simeq 1/3$ power law for the energy dependence of the diffusion coefficient [3]. The normalisation D_0 is only weakly constrained using measurements of stable nuclei, since the grammage scales as $X \propto (H/h) \times h^2/D = hH/D$ with the height of the CR halo H and the height of the matter disc h . Therefore a larger value of D_0 can be compensated by an increase of the CR halo size H . This degeneracy can be broken considering the ratio of radioactive isotopes as, e.g., $^{10}\text{Be}/^9\text{Be}$: Fitting successfully these ratios requires a relatively large CR halo, $H \simeq 5$ kpc, which in turn leads to relatively large values of the normalisation constant $D_0 = (3-8) \times 10^{28} \text{cm}^2/\text{s}$ at $E_0 = 10$ GeV [4].

At the fundamental level, charged particles scatter on inhomogeneities of the Galactic magnetic field (GMF). For a given GMF model, the trajectories of charged particles can be calculated and the diffusion coefficients can be determined numerically [5–10]. The authors of the recent study Ref. [11] devised a theory allowing to calculate analytically the diffusion coefficient in different energy ranges, for isotropic turbulence with no regular field, and they confronted it with numerical simulations. Since calculations are computationally expensive,

they are usually restricted to energies above 10^{14} eV. On the other hand, empirical diffusion models are applied mainly below 10^{13} eV. This missing overlap in energy may be the reason why—except for a few cases—a confrontation of the two methods and their conclusions seems to be missing in the literature. We noted earlier in Ref. [9] that the diffusion coefficient calculated numerically in a pure random field with $B_{\text{rms}} = 4 \mu\text{G}$ is smaller than the one extrapolated in the diffusion picture from lower energies. In Refs. [12, 13], we showed that the grammage crossed by CRs in the original Jansson-Farrar model [14] for the GMF is a factor of a few to 10 too large. The aim of the present work is to investigate these discrepancies in more detail. In particular, we want to determine qualitatively those properties of a GMF model which determine if the resulting CR propagation can be reconciled with the results obtained in diffusion models. We examine therefore several toy models which allow us to isolate some key properties a successful GMF model should possess.

This article is structured as follows: We start summarising in Sec. 2 how we model magnetic fields, propagate CRs and calculate from their trajectories the diffusion tensor. Then we investigate in Sec. 3 various toy models and derive the corresponding diffusion coefficients. Finally, we discuss the impact of anisotropic diffusion on Galactic CR physics and summarise additional evidence disfavouring the traditional steady-state picture in Sec. 4 before we conclude.

2 Theoretical framework

The GMF consists of a regular component which is ordered on kpc scales and of a turbulent field. On sufficiently small scales, the regular part can be approximated as a uniform field and we will therefore not consider specific GMF models. The turbulent component is usually modelled as a Gaussian random field; such a field is fully characterised by its power spectrum $\mathcal{P}(\mathbf{k})$. Several theoretical models, such as that of Ref. [15] for incompressible Alfvénic turbulence, suggest that the turbulence can be anisotropic. We consider therefore both isotropic and anisotropic turbulence. We assume the turbulence to be static, and consider power laws $\mathcal{P}(k) \propto N k^{-\alpha}$ for its power spectrum. The first assumption is well justified for the purpose of the present paper: Both the Alfvén velocity v_A and the velocity of the interstellar medium u are of the order of tens of km/s, which only induces negligible changes on the length and time scales considered here. Motivated by the consistency of the slope of the B/C ratio with Kolmogorov turbulence, we choose $\alpha = 5/3$ as index of the power spectrum, i.e. we set $\mathcal{P}(k) \propto k^{-5/3}$.

The fluctuations in the turbulent magnetic field extend over a large range of scales, from the dissipation scale $L_{\text{min}} \sim 1 \text{ AU}$ to the outer scale L_{max} , which varies from $L_{\text{max}} \sim 10 \text{ pc}$ in the disc to $L_{\text{max}} \sim 150 \text{ pc}$ in the halo [16]. We note that, for Kolmogorov turbulence, the coherence length L_{coh} and the outer scale L_{max} are connected by $L_{\text{coh}} = L_{\text{max}}/5$. In order to cope with this large range of length scales, we construct the magnetic field in our numerical simulations either on nested grids as described in Ref. [8] or as the sum of circularly polarised plane waves following the approach of Ref. [17]. Both methods allow us to choose the effective minimum scale L'_{min} of fluctuations in the field sufficiently small compared with the Larmor radius $R_{L,\text{low}} = cp_{\text{low}}/(eB)$ of the CRs with the lowest energy, cp_{low} , in each set of calculations. We always choose L'_{min} such that $L'_{\text{min}} \lesssim R_{L,\text{low}}/1.3$. For example, we use a grid with 256^3 vertices for the calculations of Fig. 3, which corresponds to a dynamical range of $L_{\text{max}}/L_{\text{min}} = 128$. In this Figure, $L_{\text{min}} = (100 \text{ pc})/128 = 0.78 \text{ pc}$, which is smaller than

the CR Larmor radius at the lowest energy considered there, $R_{L,\text{low}}(cp_{\text{low}} = 1 \text{ PeV}) = 1 \text{ pc}$ in a $1 \mu\text{G}$ field.

For the calculation of the diffusion tensor, we propagate individual CRs in a prescribed magnetic field (regular and/or turbulent) solving the Lorentz force equation. We perform the numerical simulations with the code described in Refs. [8, 18, 19]. Having obtained the trajectories $x_i^{(a)}(t)$ of N CRs with energy E , we calculate the diffusion tensor as

$$D_{ij}(E) = \lim_{t \rightarrow \infty} \frac{1}{2Nt} \sum_{a=1}^N x_i^{(a)} x_j^{(a)}. \quad (2.1)$$

For sufficiently large times t , such that CRs propagate over several coherence lengths, the RHS becomes time-independent. Diagonalising then the tensor D_{ij} , it can be written as $D_{ij} = \text{diag}\{D_{\perp}, D_{\perp}, D_{\parallel}\}$ where D_{\parallel} denotes the component aligned with the large-scale field.

3 Diffusion tensor and magnetic field models

3.1 Pure isotropic turbulent field

It is often assumed that the turbulent component of the GMF dominates over the regular one, $B_{\text{rms}} \gg B_0$. In a first approach, we set therefore the regular field B_0 to zero and consider a purely turbulent magnetic field. In the diffusion picture, one can model the propagation of CRs as a random walk with an energy dependent effective step size. For a pure isotropic random field, one expects therefore as functional dependence of the diffusion coefficient

$$D = \frac{cL_0}{3} [(R_L/L_0)^{2-\alpha} + (R_L/L_0)^2], \quad (3.1)$$

where the condition $R_L(E) = L_0$ determines the transition from small-angle scattering with $D(E) \propto E^2$ to large-angle scattering with $D(E) \propto E^{2-\alpha}$. At even higher energies, CRs enter the ballistic regime and the concept of a diffusion coefficient becomes ill-defined.

In Fig. 1, we show the diffusion coefficients numerically calculated using Eq. (2.1) for three different magnetic field strengths B_{rms} . The turbulent field was modelled as a homogeneous, isotropic Gaussian random field following a Kolmogorov power-spectrum $\mathcal{P}(k) \propto k^{-5/3}$ with $L_{\text{max}} = 25 \text{ pc}$. We note first that the scaling of the diffusion coefficient with energy and magnetic field strength expected from Eq. (3.1) is numerically reproduced. In particular, the two regimes, i.e. the transition from $\beta = 1/3$ to $\beta = 2$ can be clearly seen. The transition scale L_0 should scale with the coherence length as $L_0 \propto L_{\text{coh}}$, but the proportionality factor has to be determined numerically. We find that $L_0 \simeq L_{\text{coh}}/(2\pi)$ provides a good fit to our numerical results, which agrees with the findings of Ref. [5]. Having determined L_0 , we can extrapolate $D(E)$ to low energies and/or large coherence lengths, and compare it to the values found by fitting secondary ratios like B/C.

Requiring that the diffusion coefficient lies in the range $D = D_0 = (3-8) \times 10^{28} \text{ cm}^2/\text{s}$ at $E_0 = 10 \text{ GeV}$, we can determine the possible range of magnetic field strengths and coherence lengths. The allowed ranges of B_{rms} and L_{coh} are shown in Fig. 2, both for Kolmogorov and Kraichnan turbulence. The weak energy-dependence of $D(E) \propto E^{1/3}$ (for Kolmogorov turbulence) requires a reduction of B_{rms} by a factor $\sim 1/(100)^3 = 10^{-6}$, when keeping the coherence length L_{coh} fixed. Insisting instead on $B_{\text{rms}} \sim \text{few} \times \mu\text{G}$, the coherence length L_{coh} would have to be comparable to the size of the Galactic halo.

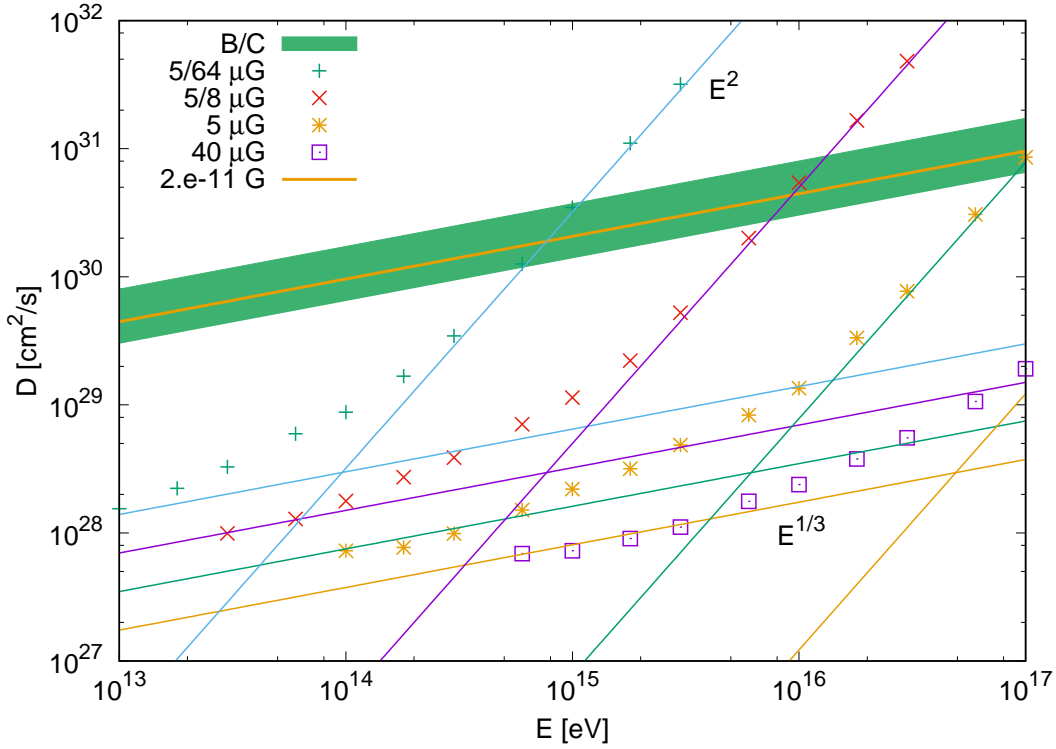


Figure 1. CR diffusion coefficient in pure isotropic Kolmogorov turbulence with $L_{\max} = 25$ pc and for four values of the turbulence root-mean-square strength: $B_{\text{rms}} = 40 \mu\text{G}$, $5 \mu\text{G}$, $(5/8) \mu\text{G}$, and $(5/64) \mu\text{G}$ —see key for symbols. The asymptotic behaviours at low and high energies are shown with the solid lines. The lines $\propto E^{1/3}$ differ by a factor $8^{1/3} = 2$ in normalization. We also plot, in orange, the extrapolated asymptotic low-energy behaviour for $B_{\text{rms}} = 2 \times 10^{-5} \mu\text{G}$. It lies within the range of magnetic field strengths that satisfy $D_0 = (3 - 8) \times 10^{28} \text{cm}^2/\text{s}$ at $E_0 = 10 \text{GeV}$, assuming a “Kolmogorov” extrapolation to high energies (B/C constraints from Refs. [1, 2], green area).

These results demonstrate that the propagation of Galactic CRs cannot be described as isotropic diffusion: For reasonable values of the strength and coherence length of a dominantly turbulent isotropic field, CRs reside too long in the Galactic disc, overproducing therefore secondary nuclei like boron. This problem can be avoided, if the regular field is sufficiently strong, such that the diffusion parallel to this regular field becomes considerably faster than in the isotropic diffusion picture. Additionally, the turbulence itself may be anisotropic, which can further increase the parallel diffusion coefficient of CRs. Then the strongly anisotropic propagation of CRs leads to a more effective escape of CRs from the Galaxy.

3.2 Isotropic turbulence with a uniform regular field

We add next a uniform magnetic field directed along the z direction to the isotropic turbulent field. As a result, the propagation of CRs becomes anisotropic, leading to a diffusion tensor with $D_{ij} = \text{diag}\{D_{\perp}, D_{\perp}, D_{\parallel}\}$ and $D_{\parallel} > D_{\perp}$. Figure 3 shows D_{\parallel} (solid lines) and D_{\perp} (dashed lines) for six values of the level of turbulence $\eta = B_{\text{rms}}/B_0$: $\eta = 0.1$ (red lines), 0.5 (orange), 1 (green), 2 (blue), 4 (purple), and ∞ . The limit $\eta \rightarrow \infty$ corresponds to isotropic turbulence, and thence isotropic diffusion. The total magnetic field strength is chosen as $B_{\text{tot}} = \sqrt{B_{\text{rms}}^2 + B_0^2} = 1 \mu\text{G}$, and the outer scale of the turbulence is set to $L_{\max} = 100$ pc. Decreasing η , the difference between D_{\parallel} and D_{\perp} increases, while keeping the order $D_{\parallel} >$

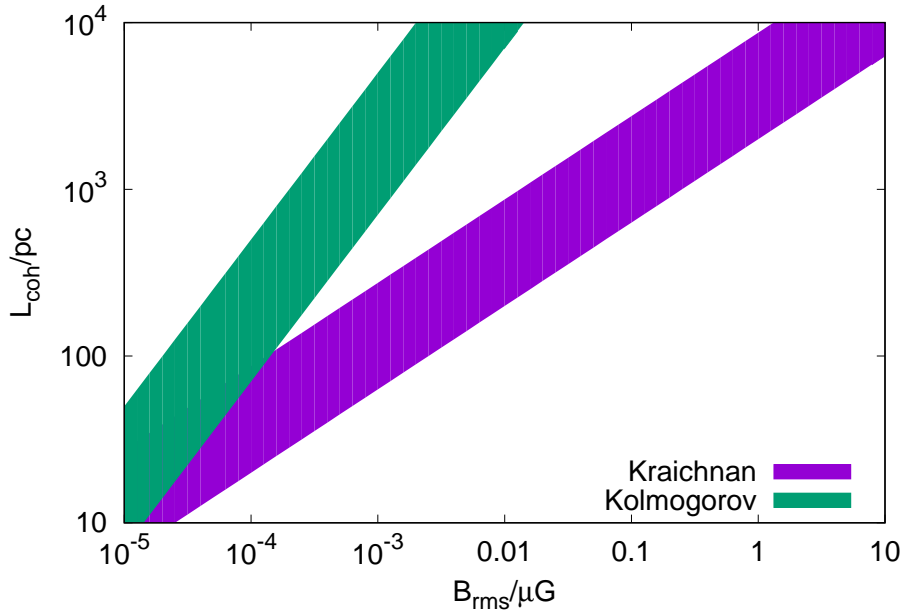


Figure 2. Allowed ranges of B_{rms} and L_{coh} compatible with $D_0 = (3-8) \times 10^{28} \text{ cm}^2/\text{s}$ at $E_0 = 10 \text{ GeV}$ for Kolmogorov and Kraichnan turbulence. These ranges should be compared with the typical order-of-magnitude values that are relevant for the Galactic magnetic field: $B_{\text{rms}} \sim (1-10) \mu\text{G}$ and $L_{\text{coh}} \lesssim$ a few tens of pc.

$D_\infty > D_\perp$ intact, where $D_\infty(E)$ denotes the diffusion coefficient for pure isotropic turbulence. We note, as previously pointed out by [7, 22], that the slope of D_\perp is larger than $1/3$ —it is close to $1/2$. Assessing whether this slope continues down to GeV energies or not is difficult due to the limited energy range one can probe. If it does, this would only make perpendicular diffusion even less relevant for the escape of CRs from the Galaxy.

Next we want to connect these results with measurements such as the B/C ratio which constrain the grammage crossed by CRs before escape. The level of turbulence η that is required to satisfy constraints from the grammage depends on the geometry of the regular Galactic magnetic field. We note that $D_\perp < D_\infty$, and that the perpendicular diffusion coefficient is therefore too small at any value of η to accommodate for a perpendicular escape of CRs in the halo, with a purely toroidal regular Galactic magnetic field.

For the sake of the argument, let us start with the simple, limiting case where the regular field is perpendicular to the Galactic disc, and where CRs escape at a distance H in the halo, along this field. In this case, the constraints that are used in Sect. 3.1 for D_∞ can now be applied to D_\parallel . The green area in Fig. 3 corresponds to the “Kolmogorov” extrapolation ($D(E) \propto E^{1/3}$) of the value $D_0 = (3-8) \times 10^{28} \text{ cm}^2/\text{s}$, inferred from the B/C ratio at $E_0 = 10 \text{ GeV}$ by the authors of Refs. [1, 2]. One can see in Fig. 3 that cases with $\eta \geq 1$ all give too small parallel diffusion coefficients to accommodate for the value required by the boron-to-carbon ratio. On the contrary, the parallel diffusion coefficients for cases with a strong regular magnetic field ($\eta < 1$) are able to fulfil the constraints from the B/C ratio. The solid orange line for $\eta = 0.5$ is at the required level, assuming Kolmogorov turbulence and $B_{\text{tot}} = 1 \mu\text{G}$. A slightly lower value of η would be preferred for $B_{\text{tot}} \gtrsim 4 \mu\text{G}$. This good

match between the diffusion coefficient required from the B/C ratio and D_{\parallel} for $\eta = 0.5$ assumes however that the regular field in the halo is perpendicular to the Galactic plane. In reality, this field is more likely to be at an angle ϑ to the plane, such as e.g. for the “X-field” in the GMF model of Ref. [14]. If so, CRs have to travel longer distances along the regular field before escape, and therefore lower values of η would be required.

In order to constrain this case quantitatively, we consider the following toy model: We assume a thin matter disc with density $\rho/m_p \simeq 1/\text{cm}^3$ and height $h = 150 \text{ pc}$ around the Galactic plane. Cosmic rays propagate inside a larger halo of height $H = 5 \text{ kpc}$. The regular magnetic field inside this disc and halo has a tilt angle ϑ with the Galactic plane, so that the component of the diffusion tensor relevant for CR escape is given by

$$D_z = D_{\perp} \cos^2 \vartheta + D_{\parallel} \sin^2 \vartheta. \quad (3.2)$$

Using a simple leaky-box model, the grammage follows as $X = c\rho h H/D_z$. Using now as allowed region for the grammage e.g. $5 \leq X \leq 15 \text{ g/cm}^2$, the permitted region in the ϑ - η plane shown in the left panel of Fig. 4 follows. For not too large values of the tilt angle, $\vartheta \lesssim 30^\circ$, the regular field should strongly dominate, $\eta \lesssim 0.35$. Note that the grammage is a rather steep function of η . While the exact contour of the allowed region depends on the assumed parameters, the conclusion that the regular field should dominate, i.e. that η is small, does not depend on the exact values of these parameters.

Let us now consider as an example of concrete GMF model the one of Jansson and Farrar [14]. We showed in Refs. [12, 13] that one can reproduce the correct grammage CRs cross, if one reduces the turbulent field in this model by a factor $\approx 8 - 10$. We found that this yields an average turbulence level of $\eta \simeq 0.25$ along CR trajectories. CRs propagate mainly along the regular field and, since the field in this model contains a z component, CRs propagate efficiently towards the Galactic halo. In this model, $\vartheta \simeq 10.2^\circ$ at Earth, and ϑ increases further in the halo (with $\vartheta < 49^\circ$ at relevant Galactocentric radii). We estimate as a typical value for CR escape $\vartheta \approx 20^\circ$. As can be seen in Fig. 4 (left panel), such a value of ϑ is consistent with $\eta \approx 0.25$, which corresponds to the aforementioned value of turbulence level determined in Refs. [12, 13]. This agreement shows that our toy model with a tilted, uniform field in the halo provides, in a first approximation, an estimate of the required turbulence levels for a GMF model with a non-zero magnetic field component perpendicular to the Galactic plane.

In the right panel of Fig. 4, we show a fit of the diffusion coefficients D_{\parallel} and D_{\perp} from Fig. 3 at $E = 10^{15} \text{ eV}$ as a function of η . Using this fit, one may apply the same analysis as above to other toy models of the GMF geometry: For instance, one may estimate the resulting grammage in models without a z component of the regular magnetic field, where CR escape proceeds along the spiral arms towards the outer regions of the Galactic disc.

3.3 Anisotropic turbulent field

As noted above, the presence of a strong regular field such that $\eta \approx 0.3$ would solve the discrepancy between estimates of the CR diffusion coefficient from the B/C ratio and the calculations presented for pure isotropic turbulence ($\eta = \infty$). Another possible solution is that interstellar turbulent magnetic fields are anisotropic. We estimate below how much the diffusion coefficient would change depending on the level of anisotropy of the turbulence.

Let us start with a model where the anisotropic turbulence is generated in the following phenomenological way. Assuming a non-zero regular field along z , we use the same grid as in the previous Sections for isotropic turbulence, but rescale its components as: $B_z \rightarrow \sqrt{\xi} B_z$,

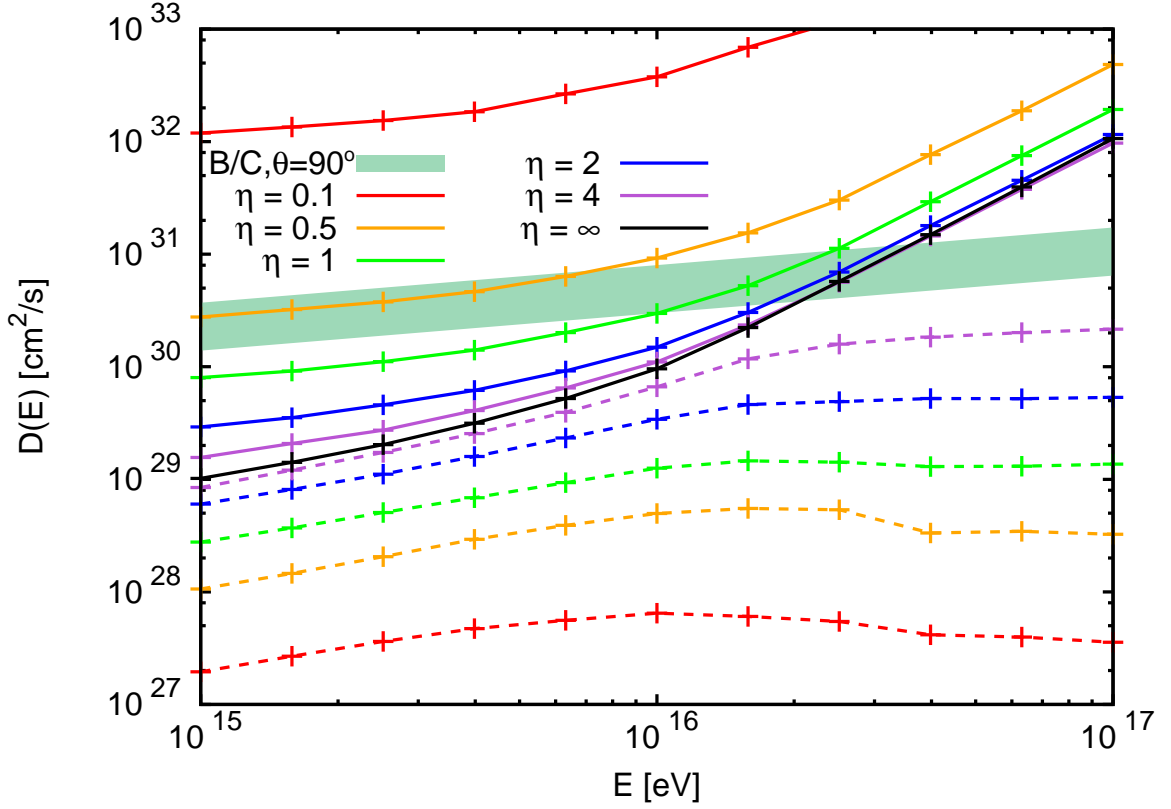


Figure 3. Parallel (solid lines) and perpendicular (dashed lines) diffusion coefficients for isotropic Kolmogorov turbulence with a superimposed regular field. Results are presented for six levels of turbulence: $\eta = 0.1$ (red lines), 0.5 (orange), 1 (green), 2 (blue), 4 (purple), ∞ (i.e. pure turbulence, black). Total magnetic field strength set to $B_{\text{tot}} = \sqrt{B_{\text{rms}}^2 + B_0^2} = 1 \mu\text{G}$, and outer scale of the turbulence equal to $L_{\text{max}} = 100 \text{ pc}$. Green area for the “Kolmogorov” extrapolation to high energies of the value $D_0 = (3 - 8) \times 10^{28} \text{ cm}^2/\text{s}$ inferred at $E_0 = 10 \text{ GeV}$ from the B/C ratio [1, 2], and relevant for the limiting case $\vartheta = 90^\circ$. See Fig. 4 (left panel) for other values of ϑ .

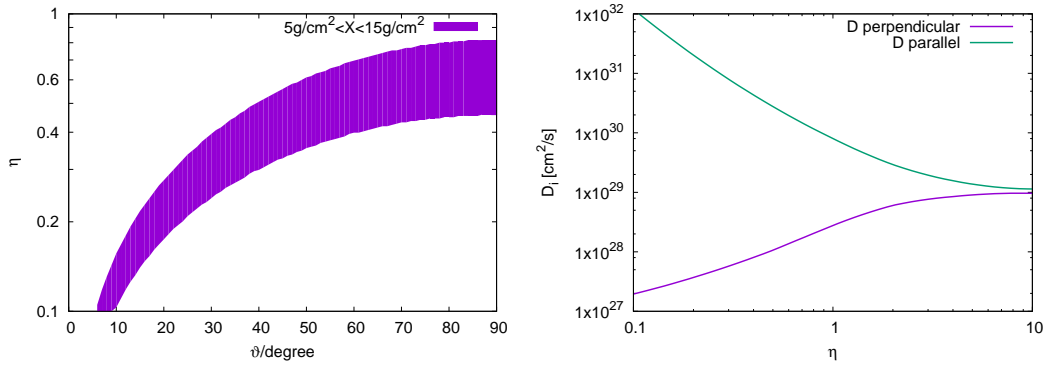


Figure 4. Left: Grammage X crossed by CRs in a “disc and halo” model, for the diffusion coefficients shown in Fig. 3, as a function of the tilt angle ϑ between the regular magnetic field and the Galactic plane, and of the turbulence level η . Right: Fit of the diffusion coefficients D_{\parallel} and D_{\perp} from Fig. 3 at $E = 10^{15} \text{ eV}$ as a function of η .

and $B_{x,y} \rightarrow \sqrt{(3-\xi)/2} B_{x,y}$, with $0 < \xi < 3$. With this prescription, the value of B_{rms} remains unchanged from that of the initial grid, while the component of the turbulent field in the direction of the regular field can be either enhanced or decreased. We have defined here the direction of the anisotropy as that of the regular field and not of local field lines. This is acceptable as long as η is small. This method has the advantages of being computationally inexpensive, providing an easy way to generate the turbulence, and giving intuitively clear results. It does not conserve $\text{div } \mathbf{B} = 0$ though, but this is unimportant for the message of the present paper. We verified on a few examples that generating anisotropic turbulence with $\text{div } \mathbf{B} = 0$ would not change results significantly: To do so, we used the method of Refs. [17], and introduced an anisotropy in Fourier space, for instance by generating wave vectors \mathbf{k} preferentially perpendicular to the regular magnetic field. This is however computationally more expensive.

In Figure 5, we present calculations of the parallel (solid lines) and perpendicular (dashed lines) diffusion coefficients with the grid method, for a turbulence level $\eta = 0.5$. The outer scale of the turbulence is set to $L_{\text{max}} = 100 \text{ pc}$, and the total magnetic field strength $B_{\text{tot}} = \sqrt{B_{\text{rms}}^2 + B_0^2}$ is equal to $1 \mu\text{G}$ in the upper panel, and $4 \mu\text{G}$ in the lower one. Five levels of anisotropy are shown: Two where the component B_z of the turbulence is reduced, $\xi = 0.0001$ (grey lines) and 0.2 (blue), and three where it is enlarged, $\xi = 2.5$ (orange lines), 2.99 (red) and 2.9999 (magenta). For reference, the case of isotropic turbulence ($\xi = 1$) is shown with the solid and dashed black lines. The thin black dotted lines in each panel correspond to $D(E) \propto E^{1/3}$, and have arbitrary normalizations. They are plotted to guide the eye, and show $1/3$ slopes.

As can be seen in Fig. 5, the value of the perpendicular diffusion coefficient does not vary significantly with ξ . On the contrary, the variations in the parallel diffusion coefficient can be substantially larger for some values of ξ . For the two cases where the turbulence is enhanced in the directions perpendicular to the regular field ($\xi = 0.0001$ and $\xi = 0.2$), both the parallel and perpendicular diffusion coefficients are reduced by a small factor, in comparison with the case of isotropic turbulence. In both panels, this reduction is quite small: no more than a factor $\simeq 2-3$, even in the extreme case of a nearly pure perpendicular geometry of the turbulence. This kind of anisotropy neither helps in increasing the diffusion coefficient, nor has a substantial impact on it.

On the contrary, for $\xi > 1$, the parallel diffusion coefficient increases in comparison with isotropic turbulence. For $\xi = 2.5$, it still has not fully reached its asymptotic $\propto E^{1/3}$ behaviour for $B_{\text{tot}} = 1 \mu\text{G}$ at the lowest energy we consider here, 10^{15} eV . However, this would happen at lower energies. Indeed, for the stronger field shown in the lower panel, the solid orange line reaches a $\propto E^{1/3}$ behaviour below $\simeq 3 \text{ PeV}$ as can be seen by comparing its slope with that of the thin black dotted line. The slope of the solid black line ($\xi = 1$) converges towards $1/3$ more quickly. It is reached below a few PeV even in the upper panel. From the lower panel, one can deduce that the normalisation of the diffusion coefficient at low energies for $\xi = 2.5$ is larger than that for $\xi = 1$ by a factor ≈ 2.7 . Such a value is however still small compared with the increase one would need in order to make the cases with $\eta \geq 2$ satisfy the constraints from the grammage, even though $\xi = 2.5$ already corresponds to a non-negligible anisotropy. We verified that even in the case of $\xi = 2.9$, D_{\parallel} is only increased by a factor of a few more compared with $\xi = 2.5$. The parallel diffusion coefficient D_{\parallel} starts for $\xi = 2.99$ to be an order of magnitude larger than for $\xi = 2.5$, see solid red lines in Fig. 5. The solid magenta lines for $\xi = 2.9999$ show that if nearly all the power of the turbulence is along B_z , then the diffusion coefficient would increase by orders of magnitude. Indeed, there is

almost no power in the two components of the turbulent magnetic field that can change the pitch-angle of the CRs, B_x and B_y . We conclude that anisotropic turbulence can alleviate the constraints put on η in Sect. 3.2, by allowing for larger turbulence levels η to satisfy the constraints from the boron-to-carbon ratio. However, a very large level of anisotropy in \mathbf{k} -space, ξ , would be needed for the difference to be substantial. Consequently, CRs would propagate also in this case strongly anisotropically.

We calculate now the grammage for $\eta = 0.5$, within the toy model with a tilted uniform field in the disc and halo described in Sect. 3.2. In Fig. 6, we plot in magenta the allowed area of ϑ - ξ parameter space that corresponds to grammages $5 \leq X \leq 15 \text{ g/cm}^2$. The left panel is for $B_{\text{tot}} = 1 \mu\text{G}$ and the right one is for $B_{\text{tot}} = 4 \mu\text{G}$. One can see from these plots that, for such a turbulence level η , strongly anisotropic fields with $\xi \gtrsim 2.5$ are required for not too extreme tilt angles $\vartheta \lesssim 35^\circ$.

Finally, we note that power-spectra in the parallel and perpendicular directions may be different. For instance, this is the case for Goldreich-Sridhar turbulence [15], where the power spectrum in the perpendicular direction is Kolmogorov-like, and that in the parallel direction is $\propto k^{-2}$. While such a type of turbulence is more isotropic on scales close to the outer scale, it becomes increasingly anisotropic at large wave-vectors. In Fig. 7, we present with red lines our numerical calculations of the parallel (solid lines) and perpendicular (dashed) diffusion coefficients for Goldreich-Sridhar turbulence with $L_{\text{max}} = 100 \text{ pc}$, and with a superimposed regular magnetic field satisfying $\eta = 0.1$ and $B_{\text{tot}} = 1 \mu\text{G}$. We use the power-spectrum suggested by Ref. [20],

$$\mathcal{P}(\mathbf{k}) \propto k_{\perp}^{-10/3} g(k_{\parallel} L_{\text{max}}^{1/3} / k_{\perp}^{2/3}), \quad (3.3)$$

with $g(y) = 1$ for $|y| < 1$ and $g = 0$ otherwise. For reference, we plot with black lines the results for isotropic Kolmogorov turbulence with the same L_{max} , η and B_{tot} . One can see that D_{\parallel} for this formulation of Goldreich-Sridhar turbulence is about an order of magnitude larger than that for isotropic Kolmogorov turbulence. On the contrary, D_{\perp} is about an order of magnitude smaller than that for isotropic turbulence. This is compatible with the expectation that CR scattering in Goldreich-Sridhar turbulence must be reduced with respect to isotropic turbulence [20]. The red and black curves do not coincide at the highest energies shown in Fig. 7 because the power-spectrum from Ref. [20] still contains some anisotropy even at small $|\mathbf{k}|$, i.e. close to the outer scale. While quasi-linear theory predicts that the parallel diffusion coefficient at low CR energies would become flatter or even increase with decreasing CR energy (see e.g. the red lines in the right panel of Fig. 11 from Ref. [21]), this effect is not observed in the energy range we probe here. The considered energies may be too high for this effect to become noticeable, or the unavoidable slight mismatch between local magnetic field lines and the direction of the anisotropy in numerical simulations may have an impact. While understanding the exact impact of anisotropic turbulence à la Goldreich-Sridhar on CR propagation clearly requires (and deserves) much more detailed numerical investigations, we may suggest that also in this case a small value of η is required to ensure fast enough CR escape.

4 Discussion

In the standard picture of CR propagation in the Galaxy, CRs are assumed to diffuse isotropically in a cylindrical box of height $2H$. This generally accepted picture implies that a large number of CR sources contribute to the CR flux detected at Earth, at least up to energies of 100 TeV, resulting in a smooth CR flux as a function of time and energy. Hereafter, we argue

that our results question this. Strongly anisotropic diffusion of CRs reduces significantly the number of CRs sources contributing to the local CR flux. After illustrating this point, we review additional evidence for the breakdown of the steady-state picture of continuous CR injection at relatively low energies, $E \sim 0.1\text{--}1\text{ TeV}$.

4.1 Number of sources contributing to the local CR flux

In order to illustrate the impact of anisotropic diffusion on the assumptions underlying Galactic CR physics, we consider as an example the number of sources contributing to the local CR flux. More specifically, we discuss inspired by Ref. [23, 24] the question if a single 2–3 Myr source can dominate the CR flux in the 10 TeV energy range. Let us assume that the source injects instantaneously 10^{50} erg in CRs with the power law $Q(E) = Q_0(E/E_0)^{-\alpha}$ and $\alpha \simeq 2.2$. We have shown in Refs. [9, 10] that the diffusion approximation can be applied once CRs have reached distances from the source that are greater than a few times L_{coh} . Observations from Refs. [42, 43] suggest that the local turbulence appears coherent within $\approx 10\text{ pc}$ from Earth, which provides an estimate of the local value of L_{coh} . Therefore, the use of the diffusion approximation is justified for a local source at the distance of interest here, 100–200 pc from Earth. At a given energy, the functional behaviour of the observed CR flux from a single source at the distance L and the age t can be divided into three regimes: For $2Dt \lesssim L^2$, the diffuse flux is exponentially suppressed, while for intermediate times it is

$$I(E) \simeq \frac{c}{4\pi} \frac{Q(E)}{V(t)} \quad (4.1)$$

with $V(t) = \pi^{3/2} D_{\perp} D_{\parallel}^{1/2} t^{3/2}$. When the diffusion front reaches the edge of the Galactic CR halo with size H , CRs start to escape. Thus in the third, final time regime, the slope of the CR intensity steepens as $I(E) \propto E^{-\alpha-1/3}$ in the case of Kolmogorov turbulence. Note that for all estimates of the type $2Dt \sim L^2$ or $2Dt \sim H^2$, the relevant component of the diffusion tensor should be used.

We consider first the standard case of isotropic diffusion. Then at the reference energy $E_* = 10\text{ TeV}$, the isotropic diffusion coefficient D_{iso} satisfying the B/C constraints equals $D_{\text{iso}}(E_*) \sim 5 \times 10^{29} \text{ cm}^2/\text{s}$. Thus the size of the diffusion front is $L(t) = \sqrt{2Dt} \simeq 2.5\text{ kpc}$ for $t = 2\text{ Myr}$. Assuming a Galactic CR halo size of $\sim 5\text{ kpc}$, we can use Eq. (4.1) to estimate the contribution of this single source to the observed CR intensity as

$$E_*^{2.8} I(E_*) \simeq 200 \text{ GeV}^{1.8} \text{ sr}^{-1} \text{ s}^{-1} \text{ m}^{-2}.$$

This corresponds only to 1/100 of the observed CR intensity at this energy. Therefore one expects that a large number of sources contribute to the local CR intensity in the case of isotropic diffusion. As a result, features of individual sources like a varying nuclear composition or maximal energies are washed out, and both the primary and secondary CR fluxes should be smooth.

Moving on to the case of anisotropic diffusion, we read from Fig. 4 using $\eta = 0.25$ and $D_{\text{iso}} \simeq 2 \times 10^{30} \text{ cm}^2/\text{s}$ valid at $E = 10^{15} \text{ eV}$ that $D_{\parallel} \simeq 5D_{\text{iso}}$, while $D_{\perp} \simeq D_{\text{iso}}/500$. Hence the volume $V(t) = \pi^{3/2} D_{\perp} D_{\parallel}^{1/2} t^{3/2}$ is reduced by $500/\sqrt{5} \simeq 200$ compared to the usually considered case of isotropic diffusion. Thus, a single source can contribute a fraction of order $\mathcal{O}(1)$ to the total CR intensity. Consequently, one expects breaks in the CR primary fluxes as a result of the varying composition and spectral shape of different sources, resulting in step-like features in the secondary ratios as discussed in Ref. [24]. Note also that the volume

V containing CRs overlaps only partially with potential observers located in the thin disc of height h : For a non-zero tilt angle ϑ , the length of the ellipsoid contained in the thin disk is limited by $\simeq h/\sin \vartheta \simeq 3h$.

4.2 Additional evidence against a steady-state CR flux

The assumption of a continuous injection of CRs is challenged by other observations too. First, a CR flux $\propto 1/E^{2.7}$ requires an injection spectrum $\propto 1/E^{2.4}$, for a $\propto E^{1/3}$ diffusion coefficient with energy dependence $\beta \simeq 1/3$ [3]. This slope significantly differs from the prediction $1/E^{2-2.2}$ of diffusive shock acceleration. Second, recent analyses of the photon flux measured by Fermi-LAT have shown a flux following a $1/E^{2.4}$ power law in the central Galaxy [25–27], i.e. a slope which is consistent with shock accelerated protons diffusing in Kolmogorov turbulence. Moreover, the CR flux deduced from photons emitted by local Giant Molecular Clouds within 1 kpc from the Sun shows a $1/E^{2.4}$ behaviour at $E < 20\text{--}40$ GeV and a variable, space-dependent softer flux at higher energies [28]. Third, the locally measured CR fluxes of nuclei have several breaks. In particular, the spectra show a softening above $\simeq 10$ GV, followed by a hardening above several hundred GV [29–34]. Finally, the slopes of the spectra dN/dR of different nuclei differ [29–31], although both acceleration and diffusion depend only on rigidity $R = cp/Z$. A possible interpretation of these measurements is that the usually assumed steady-state regime holds locally only at low energies [35], while at higher energies the contribution of individual sources becomes important. This interpretation is natural in the picture of anisotropic diffusion, since then the number of sources contributing to the local flux is strongly reduced.

There are several additional experimental signatures which suggest to abandon the steady-state regime. First, measurements of the CR dipole show a plateau of the amplitude in the energy range 1–100 TeV with an approximately constant phase [36]. This is inconsistent with simple diffusion models which predict that the anisotropy grows as function of energy as $(E/E_0)^\beta$ with $\beta \simeq 1/3$ for Kolmogorov turbulence. Second, the positron and antiproton fluxes have the same slope as the proton flux [37–40], while in the standard diffusion models they decrease relatively to the primary proton flux as $E^{-\beta}$. All these anomalies can be explained by a 2–3 Myr old local source dominating the CR flux in this energy range [23, 24, 41]. Note also that the B/C ratio found in Ref. [24] is consistent with Kolmogorov turbulence.

4.3 Possible restrictions

We note the following three possible caveats: First, we have considered throughout this work Gaussian random fields. Turbulent fields obtained in MHD simulations are however intermittent and it has been argued that this effect reduces on average the deflections of CRs scattering on magnetic irregularities [44]. This study also suggests that intermittency enhances anisotropies in the CR propagation. In order to quantify the consequences of non-Gaussian, intermittent magnetic field additional numerical studies should be performed in the future. Second, we have assumed that streaming of CRs around their sources does not have a major impact on our final conclusions. We note, however, that low-energy CRs escaping from their sources should excite the streaming instability [45–47], and thereby reduce the CR diffusion coefficient around the sources. For a study of the impact on the B/C ratio, see Ref. [48]. Any impact at the higher energies we considered in the above two subsections is questionable and strongly depends on the physical conditions around the sources, see the appendix of Ref. [10]. Third, the results presented here are derived in the limit of negligible CR advection in the halo. If a strong Galactic wind were to be present in the halo,

advection could make the effective size of the “halo” from which CRs are able to come back to the disk smaller than the usual estimates (\sim a few kpc). This would in turn reduce the normalisation of the relevant range of values that fit the B/C data. While advection should play a role at sufficiently low energies, there is no universal consensus on the presence of breaks, e.g. in the B/C ratio, that would indicate the transition to an advection-dominated regime [3]. Reference [49] suggests that an advection-dominated regime is reached at low energy. However, proof of such a regime at \sim GeV energies would still leave open the question whether a large-scale Galactic wind has an important impact on CR observables at the higher energies considered here.

5 Conclusions

We calculated the diffusion coefficients of charged cosmic rays (CR), propagating them in regular and turbulent magnetic fields by solving the Lorentz equation. We showed that CRs reside too long in the Galactic disc, if the magnetic field is dominated by an isotropic turbulent component for any reasonable combination of field-strengths B_{rms} and coherence lengths L_{coh} . As a result, CRs scattering on gas in the Galactic disc overproduce secondary nuclei like boron. Therefore propagation of Galactic CRs has to be strongly anisotropic, because of a sufficiently strong regular field, and/or an anisotropy of the turbulent field. A viable solution in our toy model, described in Section 3.2, is given by a tilted magnetic field with $\vartheta \simeq 20^\circ$ and $\eta \simeq 0.25$, resulting in $D_{\parallel}/5 \simeq 500D_{\perp} \simeq D_{\text{iso}}$ for the diffusion coefficients. As a consequence, the volume that CRs emitted by a single source occupy at intermediate times is reduced by a factor $\mathcal{O}(100)$ compared to the case of isotropic CR diffusion. Similarly, the number of sources contributing to the local CR flux is reduced and, therefore, single sources can dominate the CR flux already in the TeV energy range.

Acknowledgments

MK would like to thank the Lorentz Center for hospitality during the program “A Bayesian View on the Galactic Magnetic Field” and its participants for fruitful discussions. We thank the referee, Pasquale Blasi, for his helpful comments and suggestions.

References

- [1] V. L. Ginzburg, V. A. Dogiel, V. S. Berezhinsky, S. V. Bulanov and V. S. Ptuskin, “Astrophysics of cosmic rays,” Amsterdam, Netherlands: North-Holland (1990).
- [2] A. W. Strong, I. V. Moskalenko and V. S. Ptuskin, *Ann. Rev. Nucl. Part. Sci.* **57**, 285 (2007) [astro-ph/0701517].
- [3] M. Aguilar *et al.* [AMS Collaboration], *Phys. Rev. Lett.* **117**, 231102 (2016).
- [4] V. S. Ptuskin and A. Soutoul, *Astron. Astrophys.* **337**, 859 (1998); see also G. Jóhannesson *et al.*, *Astrophys. J.* **824**, 16 (2016) [arXiv:1602.02243 [astro-ph.HE]]. C. Evoli, D. Gaggero, D. Grasso and L. Maccione, *JCAP* **0810**, 018 (2008) Erratum: [*JCAP* **1604**, E01 (2016)] [arXiv:0807.4730 [astro-ph]].
- [5] F. Casse, M. Lemoine and G. Pelletier, *Phys. Rev. D* **65**, 023002 (2002) [astro-ph/0109223].
- [6] E. Parizot, *Nucl. Phys. Proc. Suppl.* **136**, 169 (2004) [astro-ph/0409191].
- [7] D. De Marco, P. Blasi and T. Stanev, *JCAP* **0706**, 027 (2007) [arXiv:0705.1972 [astro-ph]].

- [8] G. Giacinti, M. Kachelrieß, D. V. Semikoz and G. Sigl, JCAP **1207**, 031 (2012) [arXiv:1112.5599 [astro-ph.HE]].
- [9] G. Giacinti, M. Kachelrieß and D. V. Semikoz, Phys. Rev. Lett. **108**, 261101 (2012) [arXiv:1204.1271 [astro-ph.HE]].
- [10] G. Giacinti, M. Kachelrieß and D. V. Semikoz, Phys. Rev. D **88**, 023010 (2013) [arXiv:1306.3209 [astro-ph.HE]].
- [11] P. Subedi *et al.*, Astrophys. J. **837**, no. 2, 140 (2017) [arXiv:1612.09507 [physics.space-ph]].
- [12] G. Giacinti, M. Kachelrieß and D. V. Semikoz, Phys. Rev. D **90**, R041302 (2014) [arXiv:1403.3380 [astro-ph.HE]].
- [13] G. Giacinti, M. Kachelrieß and D. V. Semikoz, Phys. Rev. D **91**, 083009 (2015) [arXiv:1502.01608 [astro-ph.HE]].
- [14] R. Jansson and G. R. Farrar, Astrophys. J. **757**, 14 (2012); Astrophys. J. **761**, L11 (2012).
- [15] P. Goldreich and S. Sridhar, Astrophys. J. **438**, 763 (1995).
- [16] M. Iacobelli *et al.*, Astron. Astrophys. **558**, A72 (2013); see also G. Bernardi, A. G. de Bruyn, G. Harker *et al.*, Astron. Astrophys. **522**, 67 (2010); A. Ghosh, J. Prasad, S. Bharadwaj, S. S. Ali, J. N. Chengalur, Mon. Not. Roy. Astron. Soc. **426**, 3295 (2012).
- [17] J. Giacalone and J. R. Jokipii, Astrophys. J. Lett. **430**, 137 (1994); Astrophys. J. **520**, 204 (1999).
- [18] G. Giacinti, M. Kachelrieß, D. V. Semikoz and G. Sigl, JCAP **1008**, 036 (2010) [arXiv:1006.5416 [astro-ph.HE]].
- [19] G. Giacinti, M. Kachelrieß, D. V. Semikoz and G. Sigl, Astropart. Phys. **35**, 192 (2011) [arXiv:1104.1141 [astro-ph.HE]].
- [20] B. D. G. Chandran, Phys. Rev. Lett. **85**, 4656 (2000) [astro-ph/0008498].
- [21] G. Giacinti and J. G. Kirk, Astrophys. J. **835**, 258 (2017) [arXiv:1610.06134 [astro-ph.HE]].
- [22] A. P. Snodin, A. Shukurov, G. R. Sarson, P. J. Bushby and L. F. S. Rodrigues, Mon. Not. Roy. Astron. Soc. **457**, 3975 (2016) [arXiv:1509.03766 [astro-ph.HE]].
- [23] M. Kachelrieß, A. Neronov and D. V. Semikoz, Phys. Rev. Lett. **115**, 181103 (2015) [arXiv:1504.06472 [astro-ph.HE]].
- [24] M. Kachelrieß, A. Neronov and D. V. Semikoz, Phys. Rev. D **97**, no. 6, 063011 (2018) [arXiv:1710.02321 [astro-ph.HE]].
- [25] A. Neronov and D. Malyshev, arXiv:1505.07601.
- [26] R. Yang, F. Aharonian, and C. Evoli, Phys. Rev. D **93**, 123007 (2016), [arxiv:1602.04710].
- [27] F. Acero *et al.*, Astrophys. J. Suppl. **223**, 26 (2016), [arxiv:1602.07246].
- [28] A. Neronov, D. V. Semikoz and K. Ptitsyna, Astron. Astrophys. **603**, A135 (2017) [arXiv:1611.06338 [astro-ph.HE]].
- [29] O. Adriani *et al.* [PAMELA Collab.], Science **332**, 69 (2011). [arXiv:1103.4055 [astro-ph.HE]].
- [30] M. Aguilar *et al.* [AMS Collaboration], Phys. Rev. Lett. **114**, 171103 (2015).
- [31] M. Aguilar *et al.* [AMS Collaboration], Phys. Rev. Lett. **115**, 211101 (2015).
- [32] Y. S. Yoon *et al.*, Astrophys. J. **728**, 122 (2011). [arXiv:1102.2575 [astro-ph.HE]].
- [33] H. S. Ahn *et al.*, Astrophys. J. **707**, 593 (2009). [arXiv:0911.1889 [astro-ph.HE]].
- [34] Y. S. Yoon *et al.*, Astrophys. J. **839**, 5 (2017) [arXiv:1704.02512 [astro-ph.HE]].
- [35] See e.g. M. J. Boschini *et al.*, Astrophys. J. **840**, 115 (2017) [arXiv:1704.06337 [astro-ph.HE]].

- [36] G. Di Sciascio and R. Iuppa, arXiv:1407.2144 [astro-ph.HE].
- [37] O. Adriani *et al.* [PAMELA Collaboration], Nature **458**, 607 (2009) [arXiv:0810.4995 [astro-ph]]; Phys. Rev. Lett. **111**, 081102 (2013) [arXiv:1308.0133 [astro-ph.HE]].
- [38] L. Accardo *et al.* [AMS Collaboration], Phys. Rev. Lett. **113**, 121101 (2014); M. Aguilar *et al.* [AMS Collaboration], Phys. Rev. Lett. **113**, 121102 (2014).
- [39] O. Adriani *et al.* [PAMELA Collaboration], Phys. Rev. Lett. **105**, 121101 (2010).
- [40] M. Aguilar *et al.* [AMS Collaboration], Phys. Rev. Lett. **117**, 091103 (2016).
- [41] V. Savchenko, M. Kachelrieß, D.V. Semikoz, Astrophys. J. **809**, L23 (2015) [arXiv:1505.02720 [astro-ph.HE]].
- [42] P. C. Frisch *et al.*, Astrophys. J. **760**, 106 (2012) [arXiv:1206.1273 [astro-ph.GA]].
- [43] P. C. Frisch *et al.*, Astrophys. J. **814**, 112 (2015) [arXiv:1510.04679 [astro-ph.GA]].
- [44] A. Shukurov, A. Snodin, A. Seta, P. Bushby and T. Wood, Astrophys. J. **839**, L16 (2017) [arXiv:1702.06193 [astro-ph.HE]].
- [45] V. S. Ptuskin, V. N. Zirakashvili and A. A. Plessner, Adv. Space Res. **42**, 486 (2008).
- [46] M. A. Malkov, P. H. Diamond, R. Z. Sagdeev, F. A. Aharonian and I. V. Moskalenko, Astrophys. J. **768**, 73 (2013) [arXiv:1207.4728 [astro-ph.HE]].
- [47] L. Nava, S. Gabici, A. Marcowith, G. Morlino and V. S. Ptuskin, Mon. Not. Roy. Astron. Soc. **461**, no. 4, 3552 (2016) [arXiv:1606.06902 [astro-ph.HE]].
- [48] M. D’Angelo, P. Blasi and E. Amato, Phys. Rev. D **94**, 083003 (2016) [arXiv:1512.05000 [astro-ph.HE]].
- [49] R. Aloisio, P. Blasi and P. Serpico, Astron. Astrophys. **583**, A95 (2015) [arXiv:1507.00594 [astro-ph.HE]].

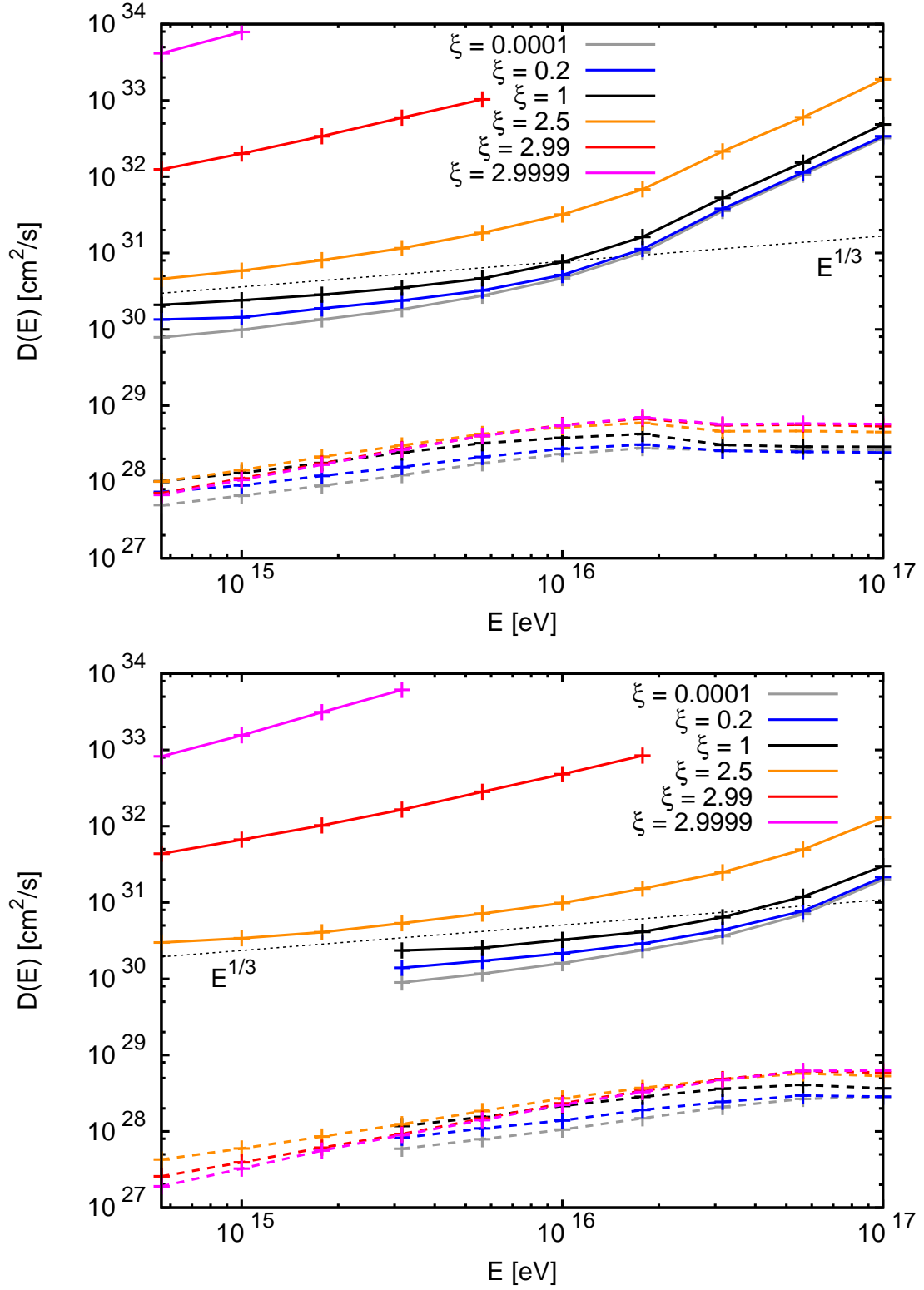


Figure 5. Parallel (solid lines) and perpendicular (dashed lines) diffusion coefficients for anisotropic turbulence with $\xi = 0.0001, 0.2, 2.5, 2.99, 2.9999$, and with a superimposed regular field satisfying $\eta = 0.5$ —see text for the definition of ξ . $L_{\text{max}} = 100 \text{ pc}$, and $B_{\text{tot}} = 1 \mu\text{G}$ (upper panel) or $4 \mu\text{G}$ (lower panel). Black line for isotropic turbulence ($\xi = 1$). Grey, blue, orange, red, and magenta lines respectively for $\xi = 0.0001, 0.2, 2.5, 2.99$, and 2.9999 . To guide the eye, the thin black dotted lines correspond to $D(E) \propto E^{1/3}$ (arbitrary normalizations).

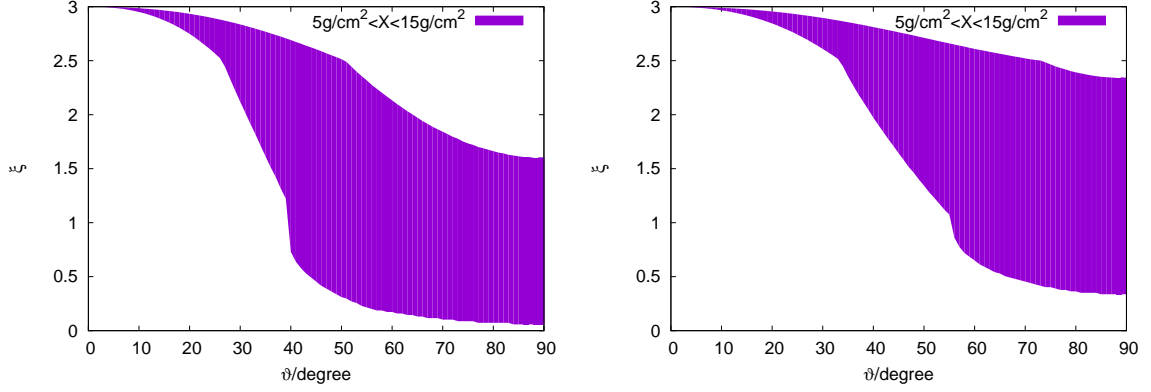


Figure 6. Grammage X crossed by CRs in a “disc and halo” model, for the diffusion coefficients shown in Fig. 5, as a function of the tilt angle ϑ between the regular magnetic field and the Galactic plane, and of the level of anisotropy ξ ; left panel for $B_{\text{tot}} = 1 \mu\text{G}$, right panel for $B_{\text{tot}} = 4 \mu\text{G}$.

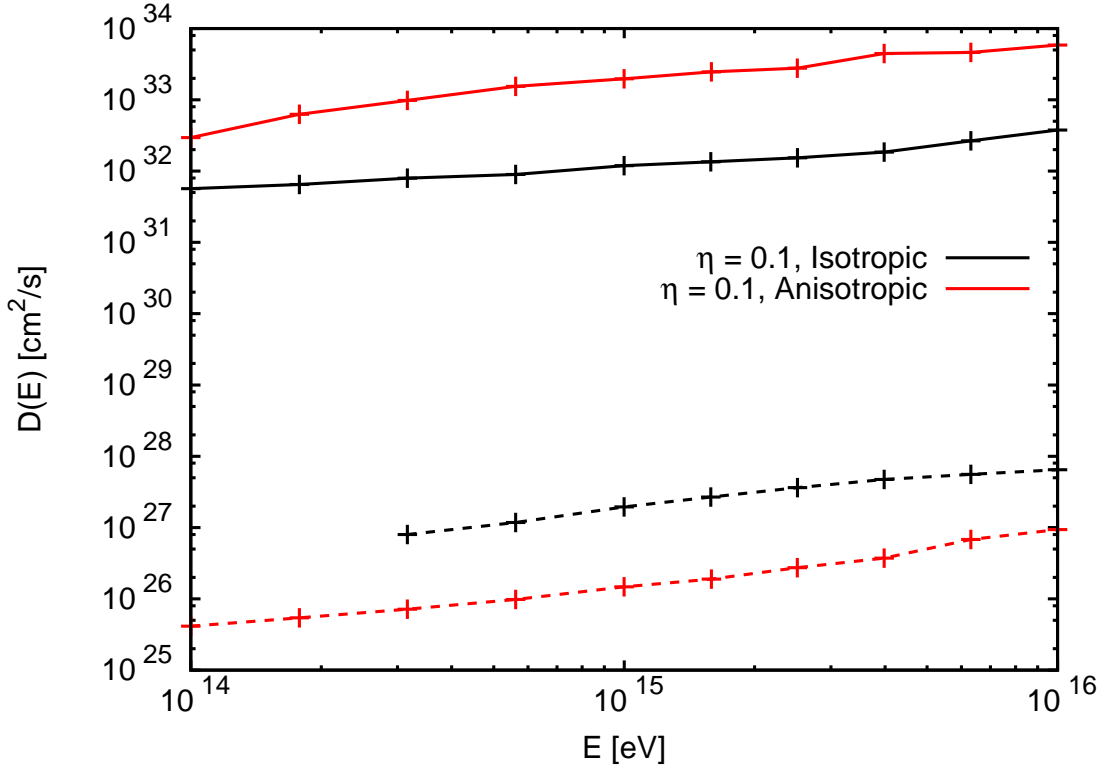


Figure 7. Parallel (solid lines) and perpendicular (dashed) diffusion coefficients for isotropic (black) and Goldreich-Sridhar (red, spectrum from Ref. [20]) turbulence, with a superimposed regular magnetic field satisfying $\eta = 0.1$. $L_{\text{max}} = 100 \text{ pc}$ and $B_{\text{tot}} = 1 \mu\text{G}$.